

EFFECT OF A CENTERED CONDUCTING BODY ON NATURAL CONVECTION HEAT TRANSFER IN AN ENCLOSURE

*John M. House, Christoph Beckermann,
and Theodore F. Smith*

*Department of Mechanical Engineering, University of Iowa,
Iowa City, Iowa 52242*

The effect of a centered, square, heat-conducting body on natural convection in a vertical square enclosure was examined numerically. The analysis reveals that the fluid flow and heat transfer processes are governed by the Rayleigh and Prandtl numbers, the dimensionless body size, and the ratio of the thermal conductivity of the body to that of the fluid. For $Pr = 0.71$ and relatively wide ranges of the other parameters, results are reported in terms of streamlines, isotherms, and the overall heat transfer across the enclosure as described by the Nusselt number. Heat transfer across the enclosure, in comparison to that in the absence of a body, may be enhanced (reduced) by a body with a thermal conductivity ratio less (greater) than unity. Furthermore, the heat transfer may attain a minimum as the body size is increased. These and other findings are justified through a careful examination of the local heat and fluid flow phenomena.

INTRODUCTION

Natural convection heat transfer in vertical rectangular enclosures has received considerable attention due to its importance in many engineering systems [1, 2]. In some instances, an obstruction may be located somewhere within the enclosure, thereby altering the natural convection flow and heat transfer. Considerable research has been performed with obstructions in the form of partitions or partial baffles [1]. However, other than the study reported by Emery [3] for a thin baffle centered vertically in the enclosure, there is little information about the natural convection processes when a solid heat conducting body is placed within the enclosure and is completely surrounded by the fluid.

In applications involving building energy components, such as walls or windows or an electronic enclosure, the body may reduce the flow, thereby reducing the heat transfer across the enclosure. On the other hand, heat transfer may be enhanced if the solid body has a relatively high thermal conductivity. In a metal casting process, a solid may be placed in the mold to form a hole in the casting. As David and Lauriat [4] noted, for a centered body with its dimensions very close to those of the enclosure, a thermal

Christoph Beckermann acknowledges partial support of the work reported in this paper by the National Science Foundation under Grant No. CBT-8808888. Computer facilities were made available by the University of Iowa WEEG Computing Center.

NOMENCLATURE

c_p	isobaric specific heat	W	size of body
g	gravitational acceleration	α	thermal diffusivity ($= k/\rho c_p$)
h	convection coefficient	β	coefficient of thermal expansion
k	thermal conductivity of fluid	ζ	dimensionless body size ($= W/L$)
k_s	thermal conductivity of body	η	dimensionless y coordinate ($= y/L$)
k^*	thermal conductivity ratio ($= k_s/k$)	θ	dimensionless temperature [$= (T - T_c)/(T_h - T_c)$]
L	spacing between hot and cold walls	μ	dynamic viscosity
Nu	Nusselt number ($= hL/k$)	ν	kinematic viscosity ($= \mu/\rho$)
P	pressure	ξ	dimensionless x coordinate ($= x/L$)
\bar{P}	dimensionless pressure ($= PL^2/\rho\alpha^2$)	ρ	density
Pr	Prandtl number ($= \nu/\alpha$)	ψ	stream function
Ra	Rayleigh number ($= g\beta \Delta TL^3/\nu\alpha$)		
T	temperature		
u	velocity in x direction		
\bar{u}	dimensionless velocity in x direction ($= uL/\alpha$)	Subscripts	
v	velocity in y direction	c	cold surface
\bar{v}	dimensionless velocity in y direction ($= vL/\alpha$)	h	hot surface
		s	solid

convection loop is obtained. On a smaller scale, understanding natural convection in an enclosure with a body may provide needed effective heat transfer data for porous media studies [5].

The purpose of this investigation is to examine the effect of a centered, square, heat-conducting body on natural convection heat transfer in a vertical square enclosure. A similar system was recently studied by David and Lauriat [4]. Their study focused primarily on the analogy of the present system with wall channeling effects in natural convection in enclosures packed with spheres. In addition, only a few detailed flow and heat transfer results were presented for the system of interest in the current study.

The system considered here is shown schematically in Fig. 1 and consists of a square enclosure with sides of length L . The left and right side walls are isothermal at respective temperatures of T_h and T_c , whereas the bottom and top walls are adiabatic. The body is centered at $L/2$, has sides of length W , and is solid with thermal conductivity k_s . The flow within the enclosure is laminar, gravitational acceleration acts parallel to the isothermal walls, and radiation effects are taken to be negligible. Except for the density in the buoyancy term, the fluid properties are assumed to be constant, and the Boussinesq approximation applies. Steady-state conditions prevail. Results of interest include the effect of the size and thermal conductivity of the solid body on the flow and temperature distributions within the enclosure and the heat transfer across the enclosure.

ANALYSIS

The steady-state conservation equations for the fluid in dimensionless form are as follows:

Continuity:

$$\frac{\partial}{\partial \xi} (\bar{u}) + \frac{\partial}{\partial \eta} (\bar{v}) = 0 \quad (1)$$

ξ Momentum:

$$\frac{\partial}{\partial \xi} (\bar{u}\bar{u}) + \frac{\partial}{\partial \eta} (\bar{u}\bar{v}) = \text{Pr} \left[\frac{\partial}{\partial \xi} \left(\frac{\partial \bar{u}}{\partial \xi} \right) + \frac{\partial}{\partial \eta} \left(\frac{\partial \bar{u}}{\partial \eta} \right) \right] - \frac{\partial \bar{P}}{\partial \xi} \quad (2)$$

η Momentum:

$$\frac{\partial}{\partial \xi} (\bar{v}\bar{u}) + \frac{\partial}{\partial \eta} (\bar{v}\bar{v}) = \text{Pr} \left[\frac{\partial}{\partial \xi} \left(\frac{\partial \bar{v}}{\partial \xi} \right) + \frac{\partial}{\partial \eta} \left(\frac{\partial \bar{v}}{\partial \eta} \right) \right] - \frac{\partial \bar{P}}{\partial \eta} + \text{Ra Pr } \theta \quad (3)$$

Energy:

$$\frac{\partial}{\partial \xi} (\bar{u}\theta) + \frac{\partial}{\partial \eta} (\bar{v}\theta) = \frac{\partial}{\partial \xi} \left(\frac{\partial \theta}{\partial \xi} \right) + \frac{\partial}{\partial \eta} \left(\frac{\partial \theta}{\partial \eta} \right) \quad (4)$$

The velocity scale used in the above dimensionless equations was chosen somewhat arbitrarily, as the ones recommended for natural convection in a vertical enclosure [2] may not apply to the present case with a centered solid body. Preliminary investigations revealed that the choice of the velocity scale had no effect on the accuracy of the numerically calculated results.

For the solid body, the energy equation is

$$0 = \frac{\partial}{\partial \xi} \left(k^* \frac{\partial \theta_s}{\partial \xi} \right) + \frac{\partial}{\partial \eta} \left(k^* \frac{\partial \theta_s}{\partial \eta} \right) \quad (5)$$

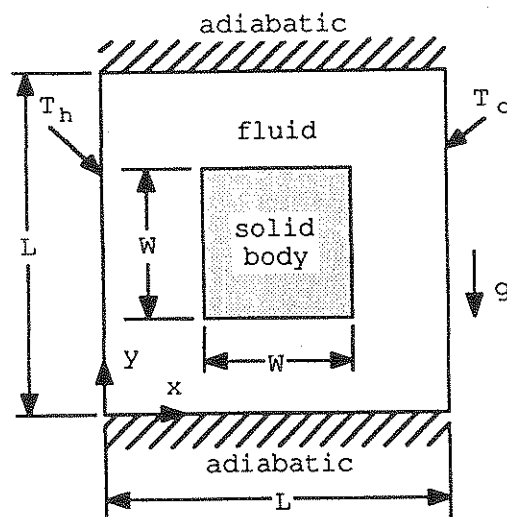


Fig. 1 Schematic of enclosure with centered solid body.

where k^* is the ratio of the thermal conductivity of the body to that of the fluid (assumed constant).

The flow boundary conditions are zero velocity at all solid surfaces. The thermal boundary conditions and the conditions at the fluid/body interface are

$$\begin{aligned} \text{At } \xi = 0: & \quad \theta = 1 \\ \text{At } \xi = 1: & \quad \theta = 0 \\ \text{At } \eta = 0 \text{ and at } \eta = 1: & \quad \frac{\partial \theta}{\partial \eta} = 0 \\ \text{At } \xi = \frac{1 - \zeta}{2} \text{ and at } \xi = \frac{1 + \zeta}{2}: & \end{aligned} \quad (6)$$

$$\theta_s = \theta \quad \frac{\partial \theta}{\partial \xi} = k^* \frac{\partial \theta_s}{\partial \xi}$$

$$\text{At } \eta = \frac{1 - \zeta}{2} \text{ and at } \eta = \frac{1 + \zeta}{2}:$$

$$\theta_s = \theta \quad \frac{\partial \theta}{\partial \eta} = k^* \frac{\partial \theta_s}{\partial \eta}$$

where $\zeta = W/L$.

The average Nusselt number is based on the enclosure width and thermal conductivity of the fluid and, for the hot wall, is expressed by

$$\text{Nu}_h = - \int_0^1 \frac{\partial \theta}{\partial \xi} \Big|_{\xi=0} d\eta \quad (7)$$

This expression without the minus sign and evaluated at $\xi = 1$ applies to the cold wall. By conservation of energy across the enclosure, the average Nusselt numbers at the hot and cold walls must be equal, that is, $\text{Nu}_h = \text{Nu}_c$.

Equations (1)–(6) reveal that there are four dimensionless parameters (Ra , Pr , k^* , ζ) that govern natural convection heat transfer in a square enclosure containing a centered square body.

NUMERICAL PROCEDURE

Numerical solutions of the governing equations were obtained using the control-volume formulation and the SIMPLER algorithm detailed in [6]. In a manner similar to that in [4] and [7], one set of conservation equations is solved over the entire domain. By setting the Prandtl number to infinity in the region occupied by the solid body, the velocities approach zero in this region. At the same locations, the dimensionless diffusion coefficient in the energy equation is changed from unity to k^* . By combining the energy equations in this manner, the matching conditions at the fluid/body interface

Table 1 Nusselt Number Comparisons for $\zeta = 0$ and $Pr = 0.71$

Ra	Present		Benchmark [8]	
	$ \psi _{\max}$	Nu	$ \psi _{\max}$	Nu
10^3	1.177	1.118	—	1.118
10^4	5.062	2.254	—	2.243
10^5	9.671	4.561	9.612	4.519
10^6	17.044	8.923	16.750	8.800

stated by Eq. (6) are satisfied automatically. The algorithm ensures continuity of the fluxes across all control surfaces and, thus, the fluid/body interface.

The harmonic mean formulation adopted for the interface diffusion coefficients between two control volumes yields physically realistic results for abrupt changes in these coefficients (that is, Pr and k^*) without requiring an excessively fine grid in the neighborhood of the fluid/body interface. Consequently, the distribution of the control volumes was only slightly skewed along all solid surfaces in order to accurately resolve large velocity and temperature gradients. Convergence of the numerical solution was checked by performing overall mass and energy balances. Most of the calculations were performed on a PRIME 9955 computer and typically required central processor times of 6000 s.

Numerical experiments were performed to establish the number of control volumes required to produce accurate results within a reasonable computational effort. First, comparisons were performed for the limiting case of no body (i.e., $\zeta = 0$) and $Pr = 0.71$ using 38 control volumes in both the ξ and η directions. As shown in Table 1, the maximum values of the stream function in the center of the enclosure and the average Nusselt numbers agree to within 1.5% with the benchmark values [8] for Rayleigh numbers up to 10^6 . Second, a grid study was performed for a medium body size (i.e., $\zeta = 0.5$) and $Pr = 0.71$. Table 2 shows the results for various thermal conductivity ratios and $Ra = 0$ and 10^5 . In these calculations, the number of control volumes in each direction was varied from 6 to 22 in the body and 8 to 24 in each passageway between the body and the enclosure walls. For all thermal conductivity ratios and Rayleigh numbers tested, the agreement between the coarse and fine grid results is excellent, which is typical of the discretization method used here. From the above two comparisons, it was decided to utilize the 38×38 control volume grid with 10×10 control volumes in the body for all calculations reported in the remainder of this article. Addi-

Table 2 Nusselt Numbers for $\zeta = 0.5$, $Pr = 0.71$, and Different Grids

k^*	Grid size					
	Ra = 0			Ra = 10^5		
	8-6-8	14-10-14	24-22-24	8-6-8	14-10-14	24-22-24
0.2	0.7051	0.7063	0.7069	4.6340	4.6239	4.6257
1.0	1.0000	1.0000	1.0000	4.5185	4.5061	4.5061
5.0	1.4098	1.4125	1.4138	4.3416	4.3249	4.3221

Table 3 Dimensionless Parameters for the Streamline and Isotherm Plots

Case	Ra	ζ	k^*	Nu
1	10^5	0.5	0.2	4.624
2	10^5	0.5	5.0	4.324
3	10^6	0.9	0.2	2.402
4	10^6	0.9	5.0	3.868

tional comparisons with the results of David and Lauriat [4] revealed agreement to within the accuracy with which their graphically presented Nusselt number data could be read.

RESULTS AND DISCUSSION

It is first instructive to examine the ranges of the governing dimensionless parameters Ra, Pr, ζ , and k^* considered in the present studies. To retain laminar flow, the Rayleigh number is kept less than or equal to 10^6 . The Prandtl number was assigned a value of 0.71. The present results may also apply to somewhat higher Prandtl numbers, as David and Lauriat [4] found that Pr has a very weak influence on the flow and heat transfer for Pr ranging from 1 to 100. The dimensionless size of the body ζ was varied from 0 to 1, where the limit of zero corresponds to pure natural convection, whereas unity represents pure conduction in the body with a resultant Nusselt number equal to k^* . Emphasis is placed on results for a thermal conductivity ratio k^* equal to 0.2 and 5.0. Physically, the latter value of k^* represents, for example, a solid body of wood in a gas with properties similar to those of air.

Streamlines and Isotherms

Streamlines and isotherms for the four cases identified in Table 3 are displayed in Figs. 2-5. These contour plots are presented in an attempt to demonstrate typical flow and heat transfer characteristics and to assist in explaining the findings for the overall Nusselt numbers (see the next section). In all cases, the streamlines show a large cell rotating clockwise about the body.

Figures 2 and 3 show the streamlines and isotherms for cases 1 and 2, where the body size is equal to 0.5. The only difference between these two cases is the value of k^* . The streamlines (Figs. 2a and 3a) are quite similar to each other. In fact, a comparison with streamlines for the case without a body (not shown here) reveals that the body has relatively little influence on the flow. This can be attributed to the fact that in pure natural convection at this Rayleigh number, the central core of the fluid region is relatively stagnant. This stagnant region approximately coincides with the bodies of cases 1 and 2. As a result, the Nusselt numbers for cases 1 and 2 (see Table 3) do not differ significantly from the corresponding pure natural convection value (see also Fig. 6).

In both cases, the isotherms (Figs. 2b and 3b) in the body are almost horizontal, indicating that heat is conducted vertically through the body, from the higher temperature fluid in the upper passage to the lower temperature fluid in the lower passage. The spacing of the isotherms in the body shows, as expected, that this effect is particularly

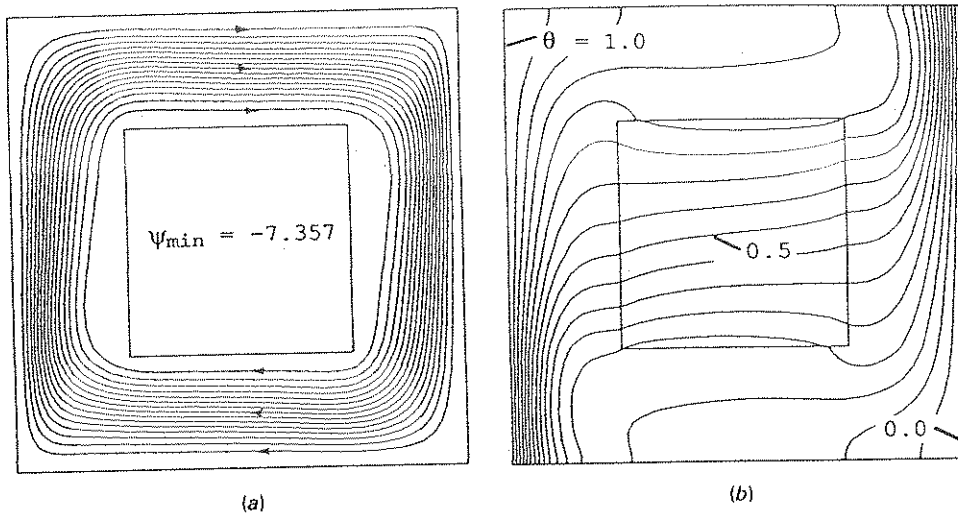


Fig. 2 Equally spaced (a) streamlines and (b) isotherms for case 1.

important for a high thermal conductivity body. Thus, for $k^* = 5$ (Fig. 3b), the hot fluid flowing in the upper passage transfers a significant portion of its sensible heat through the body to the cold fluid flowing in the lower passage instead of carrying it all the way to the cold wall of the enclosure. In turn, the cold fluid flowing in the lower passage is significantly heated by the body instead of by the hot wall of the enclosure. This "short-circuiting" by the high thermal conductivity body effectively reduces the overall natural convection heat transfer between the hot and cold walls of the enclosure.

The opposite is true for $k^* = 0.2$ (Fig. 2b). Here, the relatively low thermal conductivity body acts as an insulator between the hot and cold fluid streams in the upper

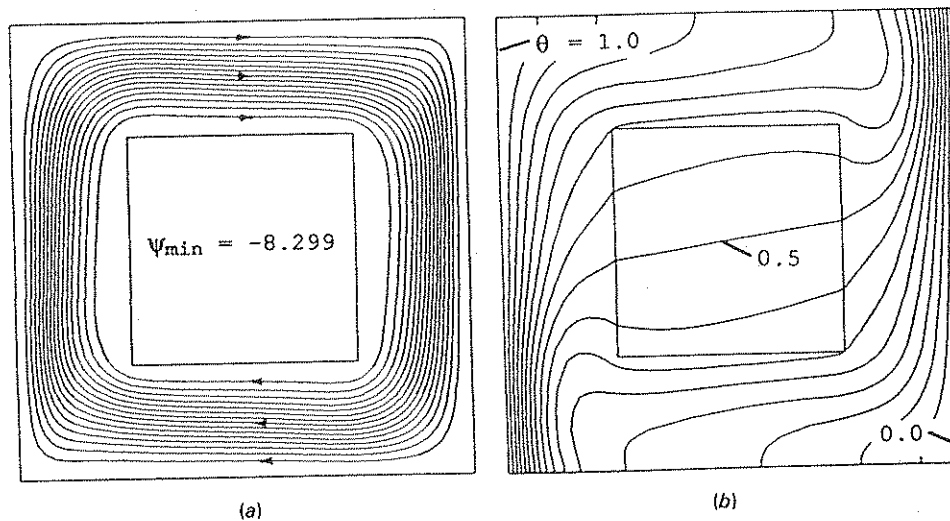


Fig. 3 Equally spaced (a) streamlines and (b) isotherms for case 2.

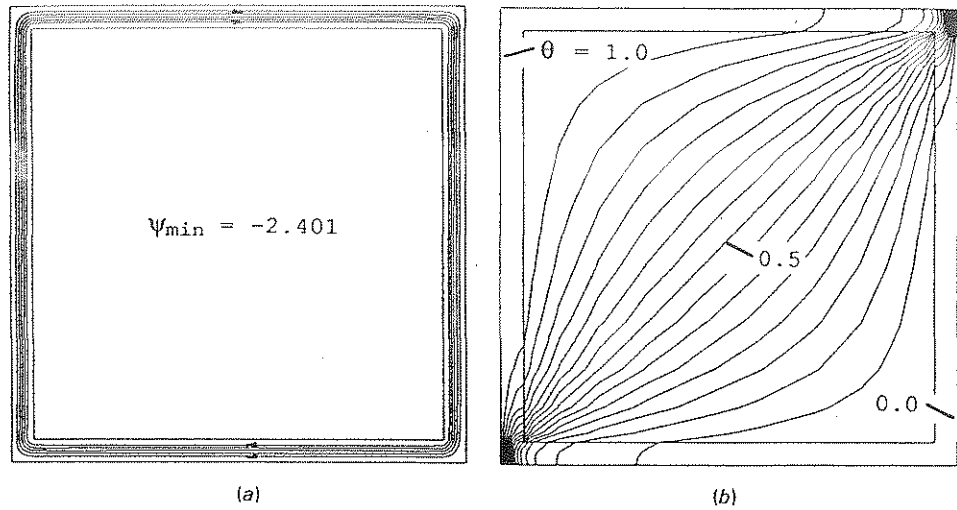


Fig. 4 Equally spaced (a) streamlines and (b) isotherms for case 3.

and lower passages. The fluid flowing between the adiabatic wall and the body experiences virtually no temperature change (see Fig. 2b). Thus, for $k^* = 0.2$, the horizontally flowing fluid advects heat more effectively between the vertical walls of the enclosure instead of losing it to or gaining it from the body as for $k^* = 5$.

The different heat transfer properties of the bodies also have an effect, albeit small, on the flow. For $k^* = 0.2$ (Fig. 2a), the streamlines near the lower left and upper right corners of the body are more separated from the vertical body walls than for $k^* = 5$ (Fig. 3a), indicating that the fluid has a higher momentum when making the 90° turn. This is due to the above-mentioned fact that the horizontally flowing fluid experiences a

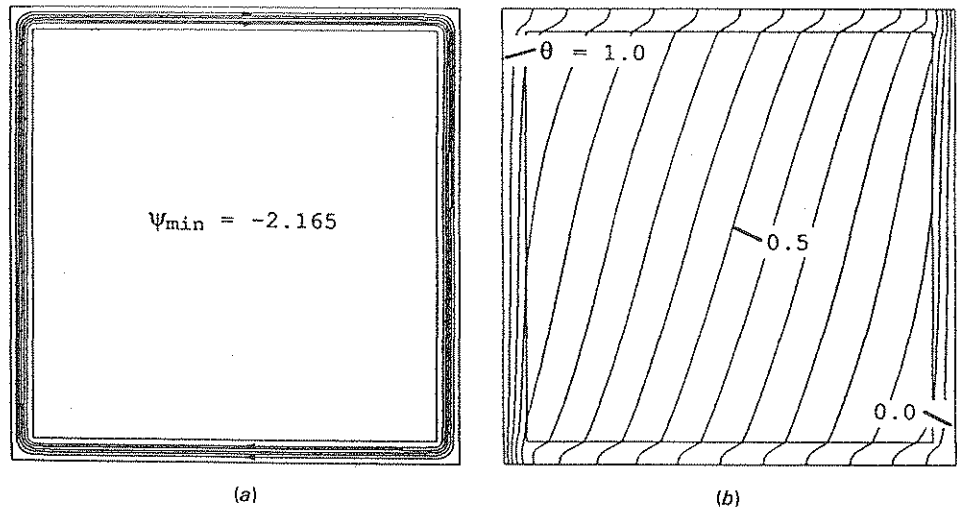


Fig. 5 Equally spaced (a) streamlines and (b) isotherms for case 4.

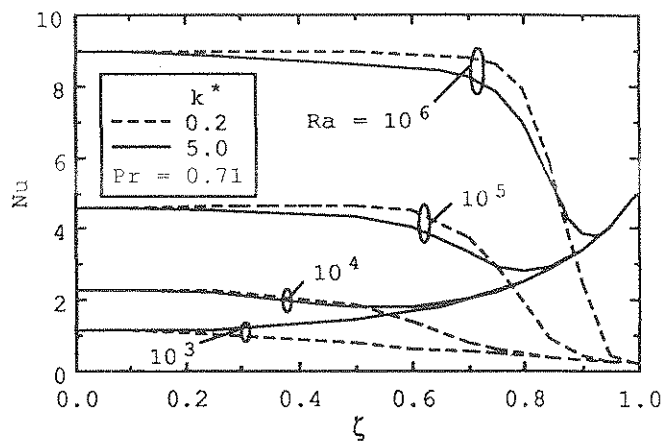


Fig. 6 Effect of Rayleigh number and thermal conductivity ratio on Nusselt number.

smaller temperature change for $k^* = 0.2$ than for $k^* = 5$, resulting in larger temperature differences between the fluid leaving the horizontal passages and the vertical walls and, hence, larger buoyancy forces. As a consequence of this separation from the body for $k^* = 0.2$, the flow is forced into more narrow regions between the body and the vertical enclosure walls, resulting in locally higher velocities and heat transfer rates at the heated and cooled walls.

The above discussion clearly shows that the combined effects of the body on the heat transfer and fluid flow are that the overall Nusselt number for $k^* = 0.2$ is higher than for $k^* = 5$ (see Table 3). In other words, a relatively low thermal conductivity body enhances the heat transfer across the enclosure, whereas a high thermal conductivity body reduces it. This result is somewhat unexpected and is only true up to a certain body size. The Nusselt number results for other body sizes, as well as comparisons with pure natural convection and conduction values, are discussed in the next section.

Streamlines and isotherms for cases 3 and 4 with $\zeta = 0.9$ are displayed in Figs. 4 and 5, respectively. Due to the large size of the body, the natural convection flow is much weaker than in cases 1 and 2 (see Figs. 4a and 5a). The streamlines for cases 3 ($k^* = 0.2$) and 4 ($k^* = 5$) appear to be almost identical. The different thermal conductivities of the bodies in cases 3 and 4 have, however, a significant influence on the isotherms in both the fluid and the body (see Figs. 4b and 5b).

For $k^* = 0.2$ (Fig. 4b), the isotherms in the fluid are highly concentrated in the lower left and upper right corners of the enclosure. The cold fluid arriving at the hot wall is heated within a short distance from the lower left corner. Then, it flows almost isothermally through the left and upper passages until it is cooled again within a short distance of the upper right corner. The cold fluid then flows almost isothermally through the right and lower passages until it reaches the lower left corner.

These peculiar heat transfer patterns can be explained as follows. As in case 1 ($k^* = 0.2$), the relatively low thermal conductivity body acts as an insulator between the hot and cold fluid in the upper and lower (as well as left and right) passages. However, there is significant heat transfer through the body from the fluid in the left (upper

passage to the fluid in lower (right) passage, particularly near the lower left and upper right corners. This is due to the fact that the thermal resistance (i.e., conduction path) across a corner is much less than that across the entire body. Because of this conduction across the lower left and upper right corners of the body, the cold (hot) fluid in the lower (upper) passage is already significantly heated (cooled) while it is approaching the hot (cold) enclosure wall. The resulting temperature increase (decrease) can clearly be seen in Fig. 4*b*. In the section of the vertical passages where the fluid flows isothermally, the heat loss (gain) of the fluid to (from) the body is balanced exactly by the heat gain (loss) from (to) the vertical wall. Although the overall heat transfer across the enclosure may be expected to be highly dominated by heat conduction through the large body, the fluid significantly augments the heat transfer by advecting heat from the lower left to the upper right corners of the enclosure. Consequently, the Nusselt number is far greater than the pure conduction value of 0.2 (see Table 3).

For $k^* = 5$ (case 4), the isotherms (Fig. 5*b*) indicate that heat transfer is almost one-dimensional across the enclosure. Due to the relatively high thermal conductivity of the body, the fluid at each position in the horizontal passages has almost the same temperature as the body bounding it. Because of the advecting nature of the horizontally flowing fluid, the isotherms in the body are slightly tilted from the vertical. On the other hand, the relatively low thermal conductivity fluid in the vertical passages acts as a thermal barrier for the heat transfer across the enclosure. This can clearly be seen from the different spacings of the isotherms in the body and the vertically flowing fluid. Overall, it can be seen that the fluid advects virtually no heat across the enclosure, and heat transfer is dominated by conduction through the vertical fluid passages and the body. Due to the large thermal resistance of the fluid in the vertical passages, the Nusselt number is significantly below the pure conduction value of 5 (see Table 3).

Nusselt Numbers

Nusselt numbers as a function of the dimensionless size of the body are shown in Fig. 6 for $Pr = 0.71$. Results are presented for $Ra = 10^3, 10^4, 10^5$, and 10^6 and $k^* = 0.2$ and 5.0. As expected, the Nusselt numbers for $k^* = 0.2$ and 5 collapse into a single value as the body size approaches zero, corresponding to pure natural convection in a vertical square enclosure. Similarly, as the body size approaches unity, the Nusselt numbers for all Rayleigh numbers collapse into a single value of k^* , corresponding to pure conduction through the body.

As discussed earlier, the body has relatively little influence on the natural convection flow, as long as it is not much larger than the almost stagnant central core present during natural convection in a vertical square enclosure without a body. Because the size of this stagnant core increases with the Rayleigh number, the value of ζ at which the body begins to significantly suppress the natural convection flow increases with Ra . As a result, the Nusselt number for $Ra = 10^3$ stays fairly close to the pure natural convection value up to only about $\zeta = 0.2$, whereas for $Ra = 10^6$ the body has only a small effect on Nu up to almost $\zeta = 0.7$ (see Fig. 6).

The above is true for both thermal conductivity ratios, although small differences can be observed. For $k^* = 0.2$ and all Rayleigh numbers, the Nusselt number first increases slightly above the pure natural convection value, reaches a maximum, and then decreases monotonically to the pure conduction value of k^* . This maximum in Nu

corresponds to a body size smaller than the size at which the body significantly suppresses the natural convection flow. The maximum can be directly attributed to the insulating nature of the body between the hot and cold fluid streams, as discussed in detail in connection with case 1. This finding implies that natural convection heat transfer for a vertical enclosure can be enhanced by inserting a relatively low thermal conductivity (and not too large) body in the center. It should be noted that for $Ra = 10^3$, this effect is not observable due to the low intensity of the natural convection flow.

For $k^* = 5$, no such maximum is present. With increasing ζ , the Nusselt number decreases continually from the pure natural convection value until it reaches a minimum. Below the value of ζ at which the body begins to significantly suppress the natural convection flow, the decrease can be directly attributed to the short-circuiting of the heat transfer by the relatively high thermal conductivity body, as discussed in detail in connection with case 2. Above that value of ζ , the decrease is steeper and is predominantly due to the suppression of the natural convection flow that is present regardless of the value of k^* . The minimum in Nu corresponds to a value of ζ at which the natural convection flow is relatively unimportant, but the vertical fluid passages still represent a major thermal resistance. Case 4, for $Ra = 10^6$, discussed in the previous section corresponds closely to that minimum. Beyond the minimum, the Nusselt number increases with ζ until it reaches the pure conduction value of $k^* = 5$, because the thickness and, thus, the thermal resistance of the vertical fluid passages decreases. As expected, for smaller Rayleigh numbers, the minimum in Nu shifts to lower values of ζ and, at $Ra = 10^3$, a minimum is not observable. It is interesting to note that the Nusselt numbers for $k^* = 5$ are consistently below the ones for $k^* = 0.2$ up to a value of ζ at which the body has already significantly suppressed the natural convection flow (see Fig. 6). This finding is generalized for other values of k^* in the following discussion of Fig. 7.

The effect of k^* on the Nusselt number is shown in Fig. 7. The values of Ra

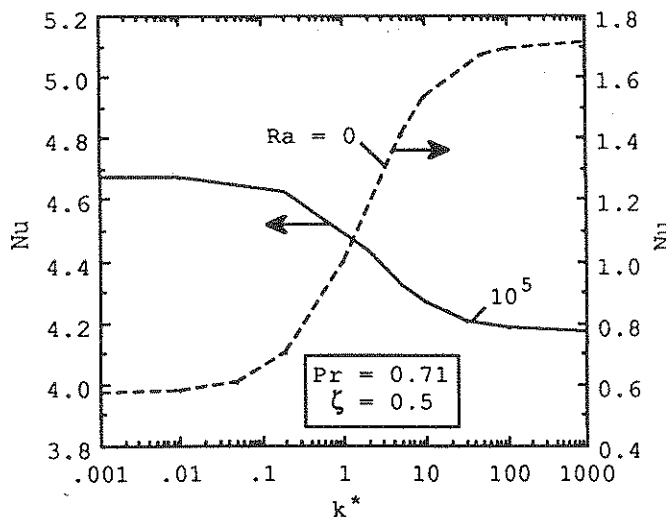


Fig. 7 Effect of thermal conductivity ratio on Nusselt number.

($= 10^5$), $Pr (= 0.71)$, and $\zeta (= 0.5)$ in Fig. 7 were chosen to illustrate the effect of k^* for a body that does not significantly suppress the natural convection flow. To demonstrate the corresponding variation of Nu with k^* that can be expected in the absence of natural convection flow, a curve for $Ra = 0$ is also included in Fig. 7. As expected, for $Ra = 0$, the Nusselt number increases monotonically with an increasing thermal conductivity ratio. The opposite, however, is true in the presence of natural convection (i.e., for $Ra = 10^5$). Here, the Nusselt number continually decreases with increasing k^* . In the limits of $k^* \rightarrow 0$ and ∞ , the Nusselt number asymptotically approaches values that are about 2.5% higher and 8.6% lower, respectively, than the corresponding Nusselt number for no body (see Table 1), whereas most of the change takes place between thermal conductivity ratios of 0.1 and 10. Again, the increase of Nu above the pure convection value can be explained by the fact that for small k^* , the body provides an insulation between the horizontally flowing hot and cold fluid streams. On the other hand, the decrease below the pure natural convection value for large k^* is mainly due to the short-circuiting of the two fluid streams by conduction vertically through the body. Another reason for a lower Nusselt number is, of course, the suppression of the flow by the body that is present regardless of the value of k^* . The latter effect is primarily responsible for the asymmetry of the Nu vs. k^* curve about the pure natural convection value (see Table 1). Figure 7 shows that the Nusselt number (for $\zeta = 0.5$) is equal to the pure natural convection value (i.e., for $\zeta = 0$) for a thermal conductivity ratio of approximately 0.45.

CONCLUSIONS

A numerical study has been performed of natural convection in a vertical square enclosure containing a centered square heat conducting body. From an examination of the heat and fluid flow phenomena revealed by the numerical experiments, the following major conclusions can be drawn:

1. The Nusselt number is not significantly different from the one for pure convection without a body at the same Rayleigh and Prandtl numbers, up to a body size that approximately coincides with the relatively stagnant fluid core present in a vertical enclosure without a body.
2. For larger body sizes, the variation of Nusselt number with body size is significantly influenced by the ratio of the thermal conductivity of the body to that of the fluid. For relatively large ratios, the Nusselt number displays a minimum at a body size at which the natural convection flow is "successfully" suppressed, but the vertical fluid passages still represent a major thermal resistance. On the other hand, for relatively low ratios, the flow in the relatively small fluid passages does play an important role and the Nusselt numbers are always above the value of the thermal conductivity ratio.
3. For smaller body sizes, the present study conclusively shows that the presence of a relatively *low* thermal conductivity body can *enhance* the heat transfer rate across the enclosure to values that are above the ones for pure natural convection without the body at the same Rayleigh and Prandtl numbers. For the same body size, a relatively *high* thermal conductivity body *reduces* the total heat transfer rate.

In summary, the results of the present study are in some respects unexpected and can have important implications in many applications. For example, considerable care needs to be taken in trying to utilize a higher thermal conductivity body to enhance the heat transfer across the enclosure, as proposed by David and Lauriat [4]. In fact, the present results may serve as a motivation to develop novel techniques for minimizing the total heat transfer rate, which is important in many building energy components. From a more fundamental point of view, it is interesting to note that the heat transfer across the enclosure (or the "effective thermal conductivity") does not need to be bounded by the limiting values for $\zeta = 0$ and 1, and may follow opposite trends, as would be expected for pure heat conduction ($Ra = 0$). Although this fundamental study revealed some of the basic heat transfer mechanisms, natural convection in enclosures containing a heat conducting body needs considerably more research attention. In particular, three-dimensional effects may be important in many practical systems, for example, if the body does not extend over the entire depth of the enclosure.

REFERENCES

1. K. T. Yang, Natural Convection in Enclosures, chap. 13, in *Handbook of Single-Phase Convection Heat Transfer*, ed. S. Kakac, R. K. Shah, and W. Aung, Wiley, New York, 1987.
2. S. Ostrach, Natural Convection in Enclosures, *ASME J. Heat Transfer*, vol. 110, pp. 1175-1190, 1988.
3. A. F. Emery, Exploratory Studies of Free-Convection Heat Transfer through an Enclosed Vertical Liquid Layer with a Vertical Baffle, *ASME J. Heat Transfer*, vol. 91, pp. 163-165, 1969.
4. E. David and G. Lauriat, Analogy between Wall Channeling Effects in Porous Media and Thermal Convection Loops, *Numer. Methods in Therm. Probl.*, vol. 6, pt. 1, pp. 476-486, 1989.
5. D. Shonnard and S. Whitaker, The Effective Thermal Conductivity for a Point-Contact Porous Medium: An Experimental Study, *Int. J. Heat Mass Transfer*, vol. 32, pp. 503-512, 1989.
6. S. V. Patankar, *Numerical Heat Transfer and Fluid Flow*, Hemisphere, Washington, D.C., 1980.
7. C. Beckermann, R. Viskanta, and S. Ramadhyani, Natural Convection in Vertical Enclosures Containing Simultaneously Fluid and Porous Layers, *J. Fluid Mech.*, vol. 186, pp. 257-284, 1988.
8. G. de Vahl Davis, Natural Convection of Air in a Square Cavity: A Bench Mark Numerical Solution, *Int. J. Numer. Methods Fluids*, vol. 3, pp. 249-264, 1983.

Received 2 January 1990

Accepted 16 February 1990